SEMARAK ILMU PUBLISHING

CFD Letters

Journal homepage:
https://semarakilmu.com.my/journals/index.php/CFD_Letters/index
ISSN: 2180-1363

Bi-directional Forced Convective Stagnation Points Flow of Oldroyd-B Liquid with Joule Heating Effects: A Finite Difference Simulations

Bilal Ahmed[1,*]

[1] College of Humanities and Sciences, University of Science and Technology of Fujairah, UAE

ARTICLE INFO

Article history:
Received 7 September 2023
Received in revised form 10 October 2023
Accepted 15 November 2023
Available online 29 February 2024

Keywords:
Oldroyd-B Fluid; Bi-Directional Flow; Joule Heating; Finite Difference Scheme

ABSTRACT

The impact of Joule heating for the three-dimensional stagnation point flow of non-Newtonian liquid (namely Oldroyd-B) nanomaterial has been inspected. The influence of mixed convection and the magnetic force is also considered. The flow is induced by the bidirectional stretched surface which moves linearly. The partial differential equations for the developed model are altered into dimensionless statements first. The numerical simulations with the implementation of a finite difference scheme are used for the numerical description. The physical description of parameters is presented against the flow parameters. The results reveal that there is a reverse change in velocity observed for both the relaxation time constant and the retardation constant. Furthermore, the heat transfer rate decreases as the ratio parameter increases. The thickness of the boundary layer increases due to the retardation time and can also be regulated by the application of a magnetic field. An increase in the magnetic parameter leads to an enhancement in temperature and an increase in thermal boundary layer thickness.

1. Introduction

The surveys concerning the impact of non-Newtonian fluids are a fascinating research field in applied engineering (fluid mechanics) and intended the attention of analysts in current century. Owing to the fundamental applications of non-Newtonian materials in various industries, petroleum industries, mechanical engineering, chemical processes, and bio-medical sciences, the understanding of such materials is quite necessary. In contrast to viscous fluids, the non-Newtonian fluids are complicated in nature. Some fluids like blood, paints, silicone oils, starch and molasses are characterized as non-Newtonian material. To study the behaviour and nature of non-Newtonian liquids, different nonlinear models are imposed by numerous researchers. Such fluids are habitually categorised in three groups, i.e., integral, differential and rate type. The considered fluid model is occurred in rate type materials. Some theoretical research regarding non-Newtonian model is classified in Ref. [1-5]. The considered model is one which efficaciously captures the interesting features of relaxation and retardation time. The results of viscous fluid and Maxwell model is

* *Corresponding author.*
E-mail address: bilalmaths7@yahoo.com (Bilal Ahmed)

https://doi.org/10.37934/cfdl.16.7.2238

obtained from Oldroyd-B model under certain limitations. Due to such motivating features of Oldroyd-B fluid, many investigators used this fluid model to examine the flow characteristics along with different features.

Khan *et al.,* [6] scrutinized the impact of rotating non-Newtonian flow and heat and mass transport by a stretchable surface. Zhang *et al.,* [7] presented the double diffusion flow of Oldroyd-B fluid over a thin film. Khan *et al.,* [8] examined the thermal diffusion characteristics of magnetized Oldroyd-B fluid which has been assumed over a sheet with stretched and accelerate with sinusoidal nature. Nonlinear couple radiated flow of non-Newtonian material with additional impact of catalytic reactions and heat generation significances was led by Wang *et al.,* [9]. Hafeez *et al.,* [10] presented a mathematical model for rotating flow of Oldroyd-B fluid induced by a rotating disk. The flow behaviour of Oldroyd-B fluid under slip mechanisms i.e., Brownian and thermophoretic diffusions is inspected by Khan *et al.,* [11] confined by an unsteady moving surface.

Manjunatha, and Choudhari [12] revealed that Velocity slip, the angle of inclination, and the presence of porous walls play a significant role in influencing the flux within an elastic tube. Salim *et al.,* [13] claimed that the Homotopy Analysis Method proves to be a robust approach for solving the MHD Jeffery-Hamel flow in the presence of a high magnetic field. Its successful application demonstrates a noteworthy alignment between the analytical and numerical results. Soid *et al.,* [14] deduced that microorganism profiles exhibit an increase as the aluminium alloy content in the upper branch increases. Conversely, they show a decrease when both the upper and lower branches have an increased titanium alloy content. Baker and Soid [15] presented the analysis of Heat Transfer Over an Exponentially Stretching/Shrinking Vertical Sheet in a Micropolar Fluid with a Buoyancy Effect and concluded that the velocity profile at the vertical plate increases with an increase in buoyancy force but decreases when micropolar effects are considered.

Shamshuddin *et al.,* [16] studied radiative Casson nanofluid flow via bidirectional stretching surface in the presence of bilateral reactions concluded that velocity of the nanofluid enhances with a higher stretching parameter and decreases with increasing Casson parameter, particularly in the horizontal x and y directions. Additionally, the skin friction coefficients decrease as the Casson parameter values increase, while maintaining specified magnetic parameter values. Ahmed *et al.,* [17] provide the analysis that involves a biaxial extending sheet with anisotropic slip conditions and discusses entropy/Bejan analysis within the context of a three-dimensional boundary layer of a hybrid nanofluid.

Shamshuddin *et al.,* [18] used a semi-analytical Chebyshev collocation scheme (CCS) is used to provide solutions of bioconvective treatment applied to a reactive Casson hybrid nanofluid flow passing over an exponentially stretching sheet. Salawu *et al.,* [19] presented the analysis of Entropy generation and current density of tangent hyperbolic of some hybridized electromagnetic nanofluid with thermal power application and established that minimizing thermal irreversibility is achieved by increasing the values of the electric field loading and magnetic field. However, entropy generation is promoted with variations in the Eckert number. Shamshuddin *et al.,* [20] carried out the analysis of thermal Péclet number, vortex viscosity, and Reynolds number on two-dimensional flow of micropolar fluid through a channel due to mixed convection and deduced that microrotation velocity of a micropolar fluid exhibits both maximum and minimum values. The thermal and solutal properties of this micropolar fluid have a significant impact on heat and mass transport rates, particularly in the context of mixed convection and buoyancy parameter effects, which enhance local heat transfer at the surface.

Cao *et al.,* [21] conducted an analysis of a fractional Oldroyd-B fluid confined between two coaxial cylinders containing gold nanoparticles. Their findings suggest that when the system is subjected to a strong magnetic field, it leads to an increase in heat transfer while simultaneously reducing the

system's velocity profile. Asjad *et al.,* [22] investigated Fractional Partial Differential Equations for MHD Casson Fluid Flow involving innovative ternary nanoparticles. They concluded that the model based on ternary nanoparticles is a more robust approach compared to hybrid and mono nanoparticles. Furthermore, they found that an increase in temperature and velocity can be achieved with larger values of fractional parameters.

Yasir *et al.,* [23] investigated the thermal and solutal transport rates, considering the Dufour and Soret effects in the flow of Oldroyd-B fluid around a stretching horizontal cylinder. Their study also considered the influence of thermophoresis particle deposition. They obtained a normalized form of the equations through similarity transformations and subsequently solved them analytically using the homotopy analysis approach in Mathematica. In other investigation, Yasir *et al.,* [24] examined the flow of Oldroyd-B nanofluid within a non-inertial frame, taking inspiration from the Cattaneo-Christov theory. They concluded that the thermal and solutal relaxation factors have a dampening effect on temperature and concentration distributions. Furthermore, due to the inclusion of elastic effects, they observed that the hydrodynamic boundary layer becomes thinner.

Finite difference approach is adopted by the numerous researchers [25-27] because of its advantage of using a uniform/non-uniform step size is that it simplifies the discretization process. Derivative approximations and difference equations are generally easier to formulate and implement when the grid is uniform. Uniform step sizes are often chosen when the geometry of the problem or the behaviour of the physical phenomena being modelled is relatively simple and regular. Finite difference method plays a crucial role in numerical simulations, modelling physical phenomena, and solving differential equations in diverse fields, making it an indispensable tool for modern scientific and engineering endeavours and utilized by numerous researchers [28-32] to simulate the different flow models.

In conclusion after the above-mentioned literature review, the motivation to study the magnetized flow of Oldroyd-B fluid over a bidirectional moving surface in the presence of Joule heating stems from its practical significance, its potential to advance various scientific fields, and its relevance in optimizing industrial processes. This research area promises to yield valuable insights and solutions that can have a far-reaching impact on both academia and industry. The flow is initiated by the uniform motion of a bidirectional stretched surface, and the resulting stagnation point pattern is modelled and investigated. A solution is obtained from transform ordinary differential equations using finite difference numerical techniques by discretizing the domain into a mesh of uniform grids. Finally, a comprehensive graphical analysis will be presented for the parameters under consideration.

2. Mathematical Formulation

Here, it is assumed that the flow of three-dimensional and one-directional magneto-hydrodynamic Oldroyd-B fluid and the transfer of heat over an impermeable stretching sheet at $z = 0$. Constant magnetic field of strength B_0 is applied perpendicular to the direction of the flow. The temperature and velocity of stretching sheet is $T_w(x) = dx$, with $d > 0$ and $u_w(x) = ax$, with $a > 0$ respectively. The external velocity of stretching sheet $u_e(x) = cx$, with $c > 0$ and attains uniform temperature T_∞ far away from the sheet. The geometry of considered problem is displayed in Figure 1.

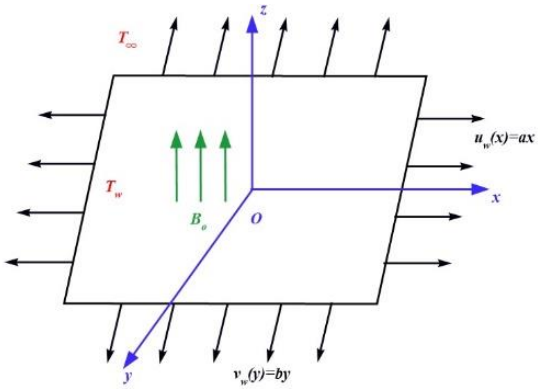

Fig. 1. Bi- dimensional flow geometry

The Cauchy stress tensor is provided in Eq. (1) which addressed as for Oldroyd-B model is taken from Sajid *et al.,* [32] is

$$\tau^{ij} = -p\delta^{ij} + S^{ij} \tag{1}$$

In which δ^{ij} highlights are identity tensor components and S^{ij} shows components of extra stress tensor, where S satisfies the following mathematical relation is provided in Eq. (2) given as;

$$\left(1 + \Lambda_1 \frac{D}{Dt}\right) S^{ij} = \mu \left(1 + \Lambda_2 \frac{D}{Dt}\right) {A_1}^{ij}, \tag{2}$$

In the Eq. (2), $\Lambda_1$is the relaxation time, ${A_1}^{ij}$ be the Rivlin-Ericksen tensor and D/Dt be the contravariant convective derivative.
For contravariant vector,

$$\frac{Db^i}{Dt} = \frac{\partial b^i}{\partial t} + v^r {b^i}_{,r} - {v^i}_{,r} b^r, \tag{3}$$

For contravariant tensor of rank 2 it gives

$$\frac{Db^{ij}}{Dt} = \frac{\partial b^{ij}}{\partial t} + v^r {b^{ij}}_{,r} - {v^i}_{,r} b^{rj} - {v^j}_{,r} b^{ir}, \tag{4}$$

Therefore ´´,`` denotes the covariant derivative, for cartesion coordinates it converted as the usual partial derivative and $v^i$are the velocity components.

By law of conservation of mass for incompressible fluids is provided in Eq. (5) given as;

$${v^i}_{,i} = 0, \qquad \text{(Equation of continuity)} \tag{5}$$

and law of conservation of momentum for present flow model is provided in Eq. (6)

$$\rho a^i = {\tau^{ij}}_{,j} + \rho b^i + \rho g \beta (T - T_\infty), \qquad \text{(Momentum equation)} \tag{6}$$

Here ρ is fluid density and a^i is the acceleration vector defined is provided in Eq. (7) as;

$$a^i = \frac{\partial a^i}{\partial t} + v^r v^i{}_{,r}, \tag{7}$$

By applying the operator $\left(1 + \Lambda_1 \frac{D}{Dt}\right)$ on Eq. (6), we get

$$\rho\left(1 + \Lambda_1 \frac{D}{Dt}\right) a^i = \left(1 + \Lambda_1 \frac{D}{Dt}\right) \tau^{ij}{}_{,j} + \rho\left(1 + \Lambda_1 \frac{D}{Dt}\right) b^i + \rho\left(1 + \Lambda_1 \frac{D}{Dt}\right) g^i \beta (T - T_\infty), \tag{8}$$

Using Eq. (1) in Eq. (8), we get

$$\rho\left(1 + \Lambda_1 \frac{D}{Dt}\right) a^i = \left(1 + \Lambda_1 \frac{D}{Dt}\right)\left(-\delta^{ij} p_{,j}\right) + \left\{\left(1 + \Lambda_1 \frac{D}{Dt}\right) S^{ij}\right\}_{,j} + \rho\left(1 + \Lambda_1 \frac{D}{Dt}\right) b^i + \rho\left(1 + \Lambda_1 \frac{D}{Dt}\right) g^i \beta (T - T_\infty), \tag{9}$$

where in obtaining Eq. (9), it is assumed that by Harris [1]

$$\left(\frac{D}{Dt}\right)_{,j} = 0 \tag{10}$$

Using Eq. (2) in Eq. (9), we get

$$\rho\left(1 + \Lambda_1 \frac{D}{Dt}\right) a^i = \left(1 + \Lambda_1 \frac{D}{Dt}\right)\left(-\delta^{ij} p_{,j}\right) + \left\{\mu\left(1 + \Lambda_2 \frac{D}{Dt}\right) A_1{}^{ij}\right\}_{,j} + \rho\left(1 + \Lambda_1 \frac{D}{Dt}\right) b^i + \left(1 + \Lambda_1 \frac{D}{Dt}\right) g^i \beta (T - T_\infty), \tag{11}$$

Again using Eq. (10), Eq. (11) becomes

$$\rho\left(a^i + \Lambda_1 \frac{Da^i}{Dt}\right) = -\left(\delta^{ij} p_{,j} + \Lambda_1 \frac{D\delta^{ij} p_{,j}}{Dt}\right) + \mu\left(A_{1,j}{}^{ij} + \Lambda_2 \frac{DA_{1,j}{}^{ij}}{Dt}\right) + \rho\left(b^i + \Lambda_1 \frac{Db^i}{Dt}\right) + \left[g^i \beta (T - T_\infty) + \Lambda_1 \frac{D}{Dt}\left(g^i \beta (T - T_\infty)\right)\right], \tag{12}$$

For steady flow, the components of velocity are defined as

$$v^1 = u(x, y, z), \quad v^2 = v(x, y, z), \quad v^3 = w(x, y, z). \tag{13}$$

Applying order of magnitude analysis, the boundary layer flow is governed by Eq. (12) and

$$u\frac{\partial u}{\partial x} + v\frac{\partial u}{\partial y} + w\frac{\partial u}{\partial z} = -\Lambda_1\left(u^2\frac{\partial^2 u}{\partial x^2} + v^2\frac{\partial^2 u}{\partial y^2} + w^2\frac{\partial^2 u}{\partial z^2} + 2uv\frac{\partial^2 u}{\partial x \partial y} + 2vw\frac{\partial^2 u}{\partial y \partial z} + 2uw\frac{\partial^2 u}{\partial x \partial z}\right) + c^2 x + \nu\frac{\partial^2 u}{\partial z^2} + \nu\Lambda_2\left(u\frac{\partial^3 u}{\partial x \partial z^2} + v\frac{\partial^3 u}{\partial y \partial z^2} + w\frac{\partial^3 u}{\partial z^3} - \frac{\partial u}{\partial x}\frac{\partial^2 u}{\partial z^2} - \frac{\partial u}{\partial y}\frac{\partial^2 v}{\partial z^2} - \frac{\partial u}{\partial z}\frac{\partial^2 w}{\partial z^2}\right) + \frac{\sigma {B^2}_0}{\rho}\left[cx - u - \Lambda_1 w\frac{\partial u}{\partial z}\right] + g\beta\left[(T - T_\infty) + \Lambda_1\left(u\frac{\partial T}{\partial x} - (T - T_\infty)\frac{\partial u}{\partial x} + v\frac{\partial T}{\partial y} + w\frac{\partial T}{\partial z}\right)\right], \tag{14}$$

$$u\frac{\partial v}{\partial x} + v\frac{\partial v}{\partial y} + w\frac{\partial v}{\partial z} = -\Lambda_1\left(u^2\frac{\partial^2 v}{\partial x^2} + v^2\frac{\partial^2 v}{\partial y^2} + w^2\frac{\partial^2 v}{\partial z^2} + 2uv\frac{\partial^2 v}{\partial x \partial y} + 2vw\frac{\partial^2 v}{\partial y \partial z} + 2uw\frac{\partial^2 v}{\partial x \partial z}\right) + c^2 x + \nu\frac{\partial^2 u}{\partial z^2} + \nu\Lambda_2\left(u\frac{\partial^3 v}{\partial x \partial z^2} + v\frac{\partial^3 v}{\partial y \partial z^2} + w\frac{\partial^3 v}{\partial z^3} - \frac{\partial v}{\partial x}\frac{\partial^2 v}{\partial z^2} - \frac{\partial v}{\partial y}\frac{\partial^2 v}{\partial z^2} - \frac{\partial v}{\partial z}\frac{\partial^2 w}{\partial z^2}\right) + \frac{\sigma {B^2}_0}{\rho}\left(cx - v - \Lambda_1 w\frac{\partial v}{\partial z}\right) + g\beta\left[\Lambda_1 (T - T_\infty)\frac{\partial v}{\partial x}\right], \tag{15}$$

The energy equation is

$$u\frac{\partial T}{\partial x}+\ v\frac{\partial T}{\partial y}+w\frac{\partial T}{\partial z}\ =\ \frac{k}{\rho c_p}\frac{\partial^2 T}{\partial z^2}+\ \frac{\mu}{\rho c_p}\left(\frac{\partial u}{\partial z}\right)^2, \tag{16}$$

The boundary conditions of the flow problem are

$$u=u_w(x)=ax,\ v=v_w(y)=by,\ \ w=0, T=T_w(x,y)=T_\infty+dxy\ \ \text{at}\ \ z=0, \tag{17}$$

$$u\to 0,\ v\to 0,\ \ \frac{\partial u}{\partial z}\to 0,\ \frac{\partial v}{\partial z}\to 0,\ \ \ T=T_\infty\ \ \ as\ \ \ z\to\infty. \tag{18}$$

where u, v & w are components of the velocity, ν is the kinematic viscosity, Λ_1 is the relaxation time, Λ_2 is the retardation time, g is the gravitational acceleration, β is the coefficient of thermal expansion, c_p specific heat, k Thermal diffusivity and T is the temperature of the fluid. Now, applying similarity transformation for a stretching flow provided in Ref. [33]

$$u=axf'(\eta),\quad v=ayg'(\eta),\quad w=-(a\nu)^{1/2}[f(\eta)+g(\eta)],\quad \theta(\eta)=\frac{T-T_\infty}{T_w-T_\infty},\quad \eta=\sqrt{\frac{a}{\nu}}z \tag{19}$$

The governing equations representing in Eq. (14) to Eq. (16) of the considered flow model are

$$f'''-f'^2+(f+g)f''+\frac{c^2}{a^2}+\lambda_1(2(f+g)f'f''-(f+g)^2f'''+A_r\theta g')+\lambda_2\Big((f''+g'')f''-(f+g)f^{iv}\Big)+M^2\left(\frac{c}{a}-f'+\lambda_1(f+g)f''\right)+A_r(\theta-\lambda_1(f+g)\theta')=0\,, \tag{20}$$

$$g'''-g'^2+(f+g)g''+\frac{c^2}{a^2}+\lambda_1(2(f+g)g'g''-(f+g)^2g''')+\lambda_2\Big((f''+g'')g''-(f+g)g^{iv}\Big)+M^2\left(\frac{c}{a}-g'+\lambda_1(f+g)g''\right)=0. \tag{21}$$

$$\theta''+Pr\big((f+g)\theta'-(f'+g')\theta\big)+PrEcf''^2=0, \tag{22}$$

And the boundary conditions resenting in Eq. (17) and Eq. (18) takes the form

$$f=0,\quad f'=1,\quad g=0,\quad g'=\frac{b}{a},\theta=1\quad \text{as}\quad \eta\to 0. \tag{23}$$

$$f'=\frac{c}{a},\quad f''=0,\quad g'=\frac{c}{a},\ \ g''=0,\quad \theta=0\quad \text{as}\quad \eta\to\infty. \tag{24}$$

Note that, prime signifies derivative w.r.t to η, $\lambda_1=\Lambda_1 a, \lambda_2=\Lambda_2 a$ the fluid parameters, $A_r=Gr/Re^2$ is the Archimedes number, $Gr=g\beta d/\nu^2$ is the Grashof number, $Re=a/\nu$ is the Reynolds number, $M^2=\sigma {B_0}^2/a\rho$ is the Hartmann number, $Pr=\mu c_p/k$ is the Prandtl number and $Ec=a^2x/dyc_p$ is the Eckert number.

3. Solution Methodology

The numerical method of boundary layer problem consisting of Eq. (20) - Eq. (22) with Eq. (23) and Eq. (24) are multiple uniform gridded by using (FDM). By and large there are two courses of action to solve boundary flow problems. The first one is coordinate transformation e.g. $\xi=1/(n+1)$is used to transform the semi-infinite physical domain $\eta\,\epsilon\,[0,\infty)$ to a finite calculation

domain $\xi \epsilon [0,1]$. In the present problem, due to the boundary condition $f' = \frac{c}{a} \quad as\ \eta \to \infty$, which relent $f' \to \infty$ as $\eta \to \infty$, in case of $c \neq 0$, a numerical approximation up to $\to \infty$ is not possible. So, method of coordinate transformation is not used. The second is method of truncating of semi-infinite domain to obtained indefinite solution. In this method the semi-infinite domain $\eta \epsilon [0, \infty)$ is replaced by finite domain $\eta \epsilon [0, L]$, the boundary condition at $\eta \to \infty$ carry out $as\ \eta = L$. We choose L in such a manner that there is no change in solution when increase the value of L.We have in view to find the numerical solution of Eq. (20) - Eq. (22) which are non-linear equations. We cannot used finite difference method for a finite domain $\epsilon[0, L]$. . Let us describe an iterative procedure determine a sequence of functions $f^{(0)}(\eta), f^{(1)}(\eta), f^{(2)}(\eta), f^{(3)}(\eta), f^{(4)}(\eta), \ldots$ and $g^{(0)}(\eta), g^{(1)}(\eta), g^{(2)}(\eta), g^{(3)}(\eta), g^{(4)}(\eta)$, … and $\theta^{(0)}(\eta), \theta^{(1)}(\eta), \theta^{(2)}(\eta), \theta^{(3)}(\eta), \theta^{(4)}(\eta), \ldots$ in the following manner. We choose $f^{(0)}(\eta), g^{(0)}(\eta)$ and $\theta^{(0)}(\eta)$ as an initial guess, then calculating the remaining successively term, from the following iterative formula

$$f'''^{(n+1)} - f'^{(n)} f'^{(n+1)} + f^{(n)} f''^{(n+1)} + g^{(n)} f''^{(n+1)} + \frac{c^2}{a^2} + \lambda_1 \left(2 f^{(n)} f'^{(n)} f''^{(n+1)} + 2 g^{(n)} f'^{(n)} f''^{(n+1)} - f^{(n)2} f'''^{(n+1)} - g^{(n)2} f'''^{(n+1)} - 2 f^{(n)} g^{(n)} f'''^{(n+1)}\right) + \lambda_2 \left(f''^{(n)} f''^{(n+1)} + f''^{(n+1)} g''^{(n+1)} - f^{(n)} f^{iv(n+1)} - g^{(n)} f^{iv(n+1)}\right) + M^2 \left(\frac{c}{a} - f'^{(n+1)} + \lambda_1 f^{(n)} f''^{(n+1)} + \lambda_1 g^{(n)} f''^{(n+1)}\right) + A_r \left(\theta^{(n)} - \lambda_1 f^{(n)} \theta'^{(n+1)} - \lambda_1 g^{(n)} \theta'^{(n+1)}\right) = 0, \quad (25)$$

$$g'''^{(n+1)} - g'^{(n)} g`^{(n+1)} + f^{(n)} g''^{(n+1)} + g^{(n)} g''^{(n+1)} + \frac{c^2}{a^2} + \lambda_1 \left(2 f^{(n)} g'^{(n)} g''^{(n+1)} + 2 g^{(n)} g'^{(n)} g''^{(n+1)} - f^{(n)2} g'''^{(n+1)} - g^{(n)2} g'''^{(n+1)} - 2 f^{(n)} g^{(n)} g'''^{(n+1)}\right) + \lambda_2 \left(f''^{(n+1)} g''^{(n+1)} + g''^{(n)} g''^{(n+1)} - f^{(n)} g^{iv(n+1)} - g^{(n)} g^{iv(n+1)}\right) + M^2 \left(\frac{c}{a} - g'^{(n+1)} + \lambda_1 f^{(n)} g''^{(n+1)} + \lambda_1 g^{(n)} g''^{(n+1)}\right) = 0, \quad (26)$$

$$\theta''^{(n+1)} + Pr \left(f^{(n)} \theta'^{(n+1)} + g^{(n)} \theta'^{(n+1)} - f'^{(n+1)} \theta^{(n)} - g'^{(n+1)} \theta^{(n)}\right) + PrEc f''^{(n)} f''^{(n+1)} = 0. \quad (27)$$

With the boundary conditions

$$f^{(n)} = 0, \quad f'^{(n+1)} = 1, \quad g^{(n)} = 0, \quad g'^{(n+1)} = \frac{b}{a}, \quad \theta^{(n)} = 1 \quad \text{as} \quad \eta \to 0 \quad (28)$$

$$f^{(n+1)} = \frac{c}{a}, \quad f''^{(n+1)} = 0, \quad g^{(n+1)} = \frac{c}{a}, \quad g''^{(n+1)} = 0 \quad \theta^{(n)} = 1 \quad \text{as} \quad \eta \to L \quad (29)$$

Which make over three linear differential equations for each iteration step $n + 1$ and might be numerically solved by applying finite difference method. It has easy to evince that if the indices (n) & $(n + 1)$ are withdrawn, the differential Eq. (25) - Eq. (27) in contact with the original differential equations Eq. (20) - Eq. (22) with boundary condition if $(L \to \infty)$. Applying central difference formulas of derivatives, Eq. (25) - Eq. (29) its becomes.

$$\left[\frac{f_{i+2} - 2f_{i+1} + 2f_{i-1} - f_{i-2}}{2h^3}\right]^{(n+1)} - \left[\frac{f_{i+1} - f_{i-1}}{2h}\right]^{(n)} \left[\frac{f_{i+1} - f_{i-1}}{2h}\right]^{(n+1)} + f_i^{(n)} \left[\frac{f_{i+1} - 2f_i + f_{i-1}}{h^2}\right]^{(n+1)} + g_i^{(n)} \left[\frac{f_{i+1} - 2f_i + f_{i-1}}{h^2}\right]^{(n+1)} + \frac{c^2}{a^2} + \lambda_1 \left(2 f_i^{(n)} \left[\frac{f_{i+1} - f_{i-1}}{2h}\right]^{(n)} \left[\frac{f_{i+1} - 2f_i + f_{i-1}}{h^2}\right]^{(n+1)} + 2 g_i^{(n)} \left[\frac{f_{i+1} - f_{i-1}}{2h}\right]^{(n)} \left[\frac{f_{i+1} - 2f_i + f_{i-1}}{h^2}\right]^{(n+1)} - f_i^{(n)2} \left[\frac{f_{i+2} - 2f_{i+1} + 2f_{i-1} - f_{i-2}}{2h^3}\right]^{(n+1)} - \right. \quad (30)$$

$$g_i^{(n)2}\left[\frac{f_{i+2}-2f_{i+1}+2f_{i-1}-f_{i-2}}{2h^3}\right]^{(n+1)}-2f_i^{(n)}g_i^{(n)}\left[\frac{f_{i+2}-2f_{i+1}+2f_{i-1}-f_{i-2}}{2h^3}\right]^{(n+1)}\Bigg)+$$
$$\lambda_2\left(\left[\frac{f_{i+1}-2f_i+f_{i-1}}{h^2}\right]^{(n)}\left[\frac{f_{i+1}-2f_i+f_{i-1}}{h^2}\right]^{(n+1)}+\left[\frac{f_{i+1}-2f_i+f_{i-1}}{h^2}\right]^{(n+1)}\left[\frac{g_{i+1}-2g_i+g_{i-1}}{h^2}\right]^{(n+1)}-\right.$$
$$\left.f_i^{(n)}\left[\frac{f_{i+2}-4f_{i+1}+6f_i-4f_{i-1}+f_{i-2}}{h^4}\right]^{(n+1)}-g_i^{(n)}\left[\frac{f_{i+2}-4f_{i+1}+6f_i-4f_{i-1}+f_{i-2}}{h^4}\right]^{(n+1)}\right)+$$
$$M^2\left(\frac{c}{a}-\left[\frac{f_{i+1}-f_{i-1}}{2h}\right]^{(n+1)}+\lambda_1 f_i^{(n)}\left[\frac{f_{i+1}-2f_i+f_{i-1}}{h^2}\right]^{(n+1)}+\lambda_1 g_i^{(n)}\left[\frac{f_{i+1}-2f_i+f_{i-1}}{h^2}\right]^{(n+1)}\right)+$$
$$A_r\left(\theta_i^{(n)}-\lambda_1 f_i^{(n)}\left[\frac{\theta_{i+1}-\theta_{i-1}}{2h}\right]^{(n+1)}-\lambda_1 g_i^{(n)}\left[\frac{\theta_{i+1}-\theta_{i-1}}{2h}\right]^{(n+1)}\right)=0,$$
$$\left[\frac{g_{i+2}-2g_{i+1}+2g_{i-1}-g_{i-2}}{2h^3}\right]^{(n+1)}-\left[\frac{g_{i+1}-g_{i-1}}{2h}\right]^{(n)}\left[\frac{g_{i+1}-g_{i-1}}{2h}\right]^{(n+1)}+f_i^{(n)}\left[\frac{g_{i+1}-2g_i+g_{i-1}}{h^2}\right]^{(n+1)}+$$
$$g_i^{(n)}\left[\frac{g_{i+1}-2g_i+g_{i-1}}{h^2}\right]^{(n+1)}+\frac{c^2}{a^2}+\lambda_1\left(2f_i^{(n)}\left[\frac{g_{i+1}-g_{i-1}}{2h}\right]^{(n)}\left[\frac{g_{i+1}-2g_i+g_{i-1}}{h^2}\right]^{(n+1)}+\right.$$
$$2g_i^{(n)}\left[\frac{g_{i+1}-g_{i-1}}{2h}\right]^{(n)}\left[\frac{g_{i+1}-2g_i+g_{i-1}}{h^2}\right]^{(n+1)}-f_i^{(n)2}\left[\frac{g_{i+2}-2g_{i+1}+2g_{i-1}-g_{i-2}}{2h^3}\right]^{(n+1)}-$$
$$\left.g_i^{(n)2}\left[\frac{g_{i+2}-2g_{i+1}+2g_{i-1}-g_{i-2}}{2h^3}\right]^{(n+1)}-2f_i^{(n)}g_i^{(n)}\left[\frac{g_{i+2}-2g_{i+1}+2g_{i-1}-g_{i-2}}{2h^3}\right]^{(n+1)}\right)+ \tag{31}$$
$$\lambda_2\left(\left[\frac{f_{i+1}-2f_i+f_{i-1}}{h^2}\right]^{(n+1)}\left[\frac{g_{i+1}-2g_i+g_{i-1}}{h^2}\right]^{(n+1)}+\left[\frac{g_{i+1}-2g_i+g_{i-1}}{h^2}\right]^{(n)}\left[\frac{g_{i+1}-2g_i+g_{i-1}}{h^2}\right]^{(n+1)}-\right.$$
$$\left.f_i^{(n)}\left[\frac{g_{i+2}-4g_{i+1}+6g_i-4g_{i-1}+g_{i-2}}{h^4}\right]^{(n+1)}-g_i^{(n)}\left[\frac{g_{i+2}-4g_{i+1}+6g_i-4g_{i-1}+g_{i-2}}{h^4}\right]^{(n+1)}\right)+$$
$$M^2\left(\frac{c}{a}-\left[\frac{g_{i+1}-g_{i-1}}{2h}\right]^{(n+1)}+\lambda_1 f_i^{(n)}\left[\frac{g_{i+1}-2g_i+g_{i-1}}{h^2}\right]^{(n+1)}+\lambda_1 g_i^{(n)}\left[\frac{g_{i+1}-2g_i+g_{i-1}}{h^2}\right]^{(n+1)}\right)=0,$$
$$\left[\frac{\theta_{i+1}-2\theta_i+\theta_{i-1}}{h^2}\right]^{(n+1)}+Pr\left(f_i^{(n)}\left[\frac{\theta_{i+1}-\theta_{i-1}}{2h}\right]^{(n+1)}+g_i^{(n)}\left[\frac{\theta_{i+1}-\theta_{i-1}}{2h}\right]^{(n+1)}-\right.$$
$$\left.\left[\frac{f_{i+1}-f_{i-1}}{2h}\right]^{(n+1)}\theta_i^{(n)}-\left[\frac{g_{i+1}-g_{i-1}}{2h}\right]^{(n+1)}\theta_i^{(n)}\right)+ \tag{32}$$
$$PrEc\left[\frac{f_{i+1}-2f_i+f_{i-1}}{h^2}\right]^{(n)}\left[\frac{f_{i+1}-2f_i+f_{i-1}}{h^2}\right]^{(n+1)}=0,$$

where $i=1,2,3,\dots,M$

Boundary conditions becomes

$$\left.\begin{aligned} f_i^{(n)}&=0, & \left[\frac{f_{i+1}-f_{i-1}}{2h}\right]^{(n+1)}&=1,\\ \left[\frac{g_{i+1}-g_{i-1}}{2h}\right]^{(n+1)}&=\frac{b}{a}, & g_i^{(n)}&=0, \end{aligned}\quad \theta_i^{(n)}=1,\quad \text{as}\quad \eta\to 0\right\} \tag{33}$$

$$\left.\begin{aligned} \left[\frac{f_{i+1}-f_{i-1}}{2h}\right]^{(n+1)}&=\frac{c}{a}, & \left[\frac{f_{i+1}-2f_i+f_{i-1}}{h^2}\right]^{(n+1)}&=0,\\ \left[\frac{g_{i+1}-g_{i-1}}{2h}\right]^{(n+1)}&=\frac{c}{a}, & \left[\frac{f_{i+1}-2f_i+f_{i-1}}{h^2}\right]^{(n+1)}&=0, \end{aligned}\quad \theta_i^{(n)}=0\quad \text{as}\quad \eta\to M.\right\} \tag{34}$$

The iterative scheme starts with the simulation with the following initial guess,

$$f_j^{(n)}=\frac{(1/2)[(c/a)-1]\eta_j^2}{\eta_M}+\eta_j,\quad g_j^{(n)}=\frac{(1/2)[(c/a)-1]\eta_j^2}{\eta_M}+\eta_j,\quad \theta_j^{(n)}=\frac{\eta_M-\eta_j}{\eta_M} \tag{35}$$

Which fulfil the boundary conditions. Now, an algebraic system of equations is solved by Gaussian elimination method at cross section $(y\epsilon[0,L])$.

4. Results and Discussion

In the recent exploration, our aim is to explicate the characteristics of mixed convection stagnation point flow of MHD of an Oldroyd-B fluid and study the physical behavior of the flow and transfer of heat. The numerical course of action described in the preceding portion for solving the governing equation of the problem is pretended by using our own built code in MATLAB & FORTRAN.

The profiles of velocity $f'(\eta), g'(\eta)$, and temperature $\theta'(\eta)$ are plotted in graphs to examine the influences of involving parameters, for example, dimensionless retardation/relaxation times (λ_1, λ_2), Hartman number M, the correspondences b/w external rate flow and stretching ratio $a\ /\ c$, the Archimedes number A_r, Prandtl number Pr and the Eckert number Ec. The physical behavior of temperature distribution $\theta(\eta)$ when several values of Eckert number Ec is considered keeping $Pr = 0.7,\ A_r = 0.1\ , c/a = 0.2, M = 0.2, \lambda_1 = 0.2, \lambda_2 = 0.2$ is shown in Table 1. Figure 2(a)-(c), describes the behavior of velocity profile $f'(\eta)$, $g'(\eta)$ of an Oldroyd-B fluid and temperature distribution $\theta(\eta)$ by taking different values of relaxation time $0.0, 0.5, 1.0, 2.0$. The relaxation time for an Oldroyd-B fluid is a crucial parameter that characterizes the viscoelastic behavior of this fluid. Oldroyd-B fluids are often used to model viscoelastic materials like polymer melts or solutions. The relaxation time characterizes the viscoelastic behavior of these fluids and represents how quickly they return to their original state after being subjected to a sudden change in stress or deformation. These figures concert the opposite behavior of momentum boundary layer and thermal boundary layer thicknesses. The velocity profile $f'(\eta)$ and $g'(\eta)$ both behave alike when relaxation time gradually grows down. Momentum boundary layer thickness is decreasing because of the relaxation time. On the other hand, temperature distribution gradually grows as relaxation time λ_1 is going to be increased.

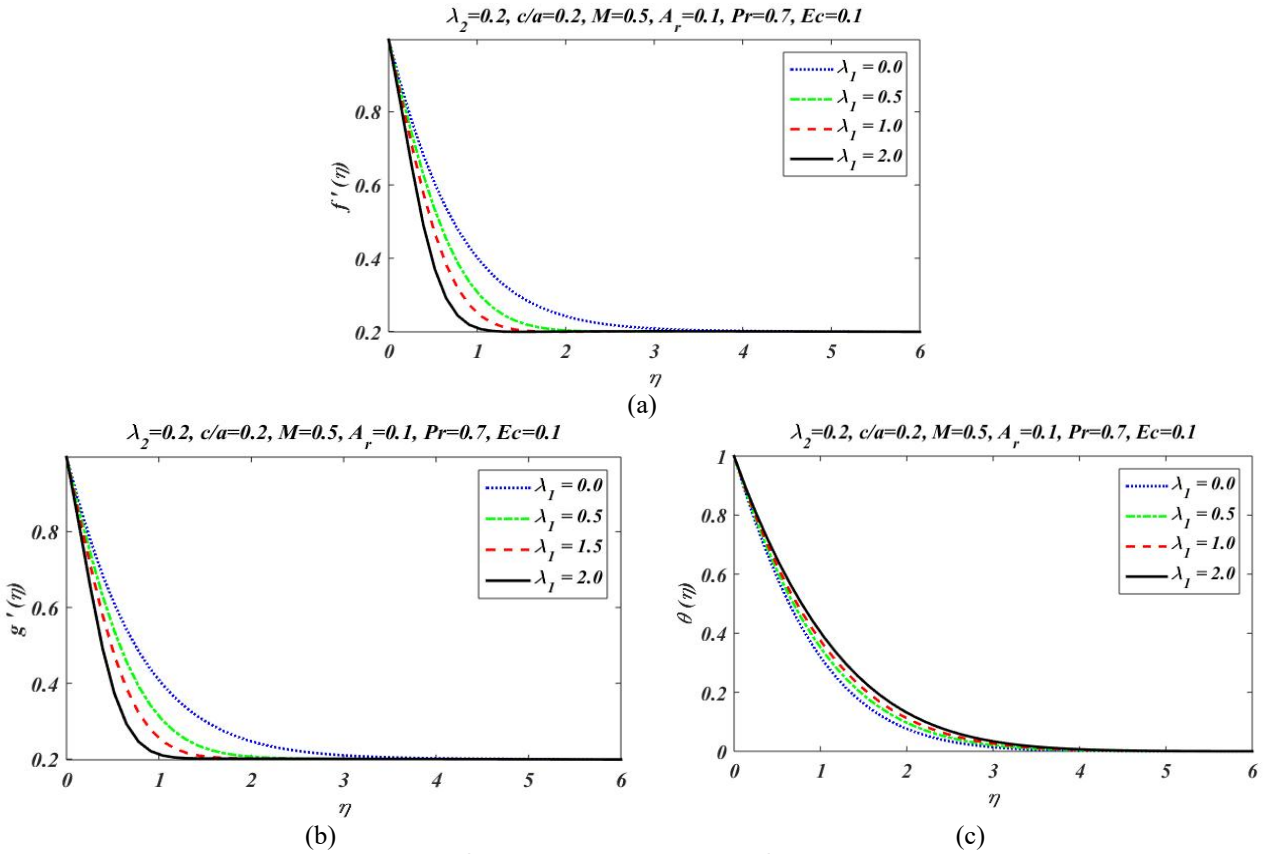

Fig. 2. Graphs of (a) Velocity profile $f^{'}(\eta)$ (b) Velocity profile $g^{'}(\eta)$ and (c) Temperature distribution $\theta(\eta)$verses η for different values of λ_1

Figure 3(a)-(c) explains the boundary layer and momentum layer thickness behavior for the different values of retardation time $\lambda_2$when relaxation time $\lambda_1 = 0.2, c/a = 0.2, A_r = 0.1, Pr = 0.7, M = 0.5, Ec = 0.1$. It is noticed that λ_2 has different behaviour as compared to that of λ_1. Velocity and momentum boundary layer thickness is increased as the retardation time is raised. The momentum boundary layer thickness is maximum at 2.0 while the thermal boundary layer thickness minimum at 2.0. It has been observed that the temperature profile become weaker as well as larger retardation time λ_2.

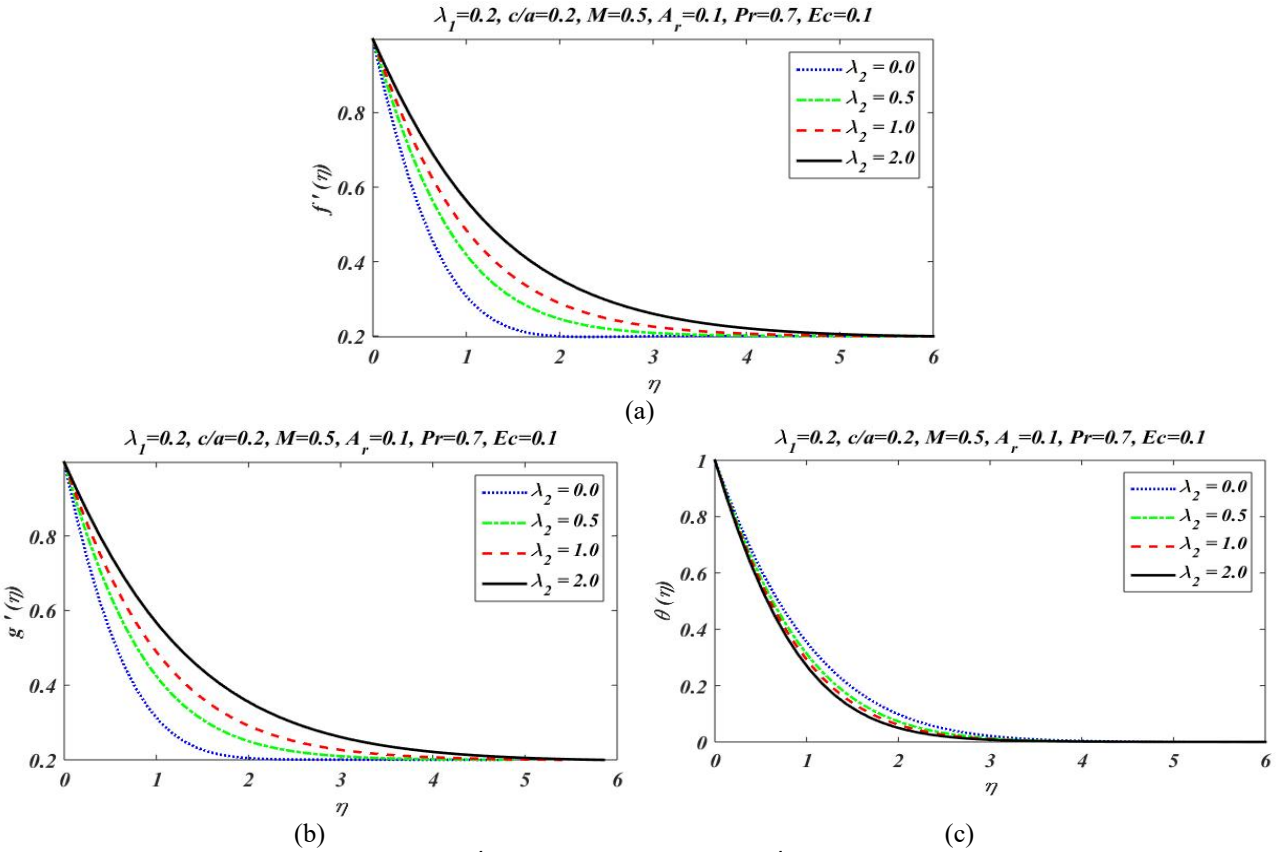

Fig. 3. Graphs of (a) Velocity profile $f'(\eta)$ (b) Velocity profile $g'(\eta)$ and (c) Temperature distribution $\theta(\eta)$ verses η for different values of λ_2

In Figure 4(a)-(c), the dimensionless parameters $Pr = 0.7, Ec = 0.1, A_r = 0.1$ and relaxation time λ_1 and retardation time λ_2 are kept constant. It is noticed that the various values of c/a assign change in the temperature distribution $\theta(\eta)$. In momentum boundary layer thickness normally, if $c/a = 1$, specifying the velocity $f'^{(\eta)}$and $g'(\eta)$ at a wall is the same as that the value aside from the wall, a deviation of the velocity from $f'(\eta) = 1$ &$g'(\eta) = 1$ happens only inside the boundary layer close to the wall. It has been also noticed that the large value of stretching ratio c/a affects the thermal boundary layer thickness.

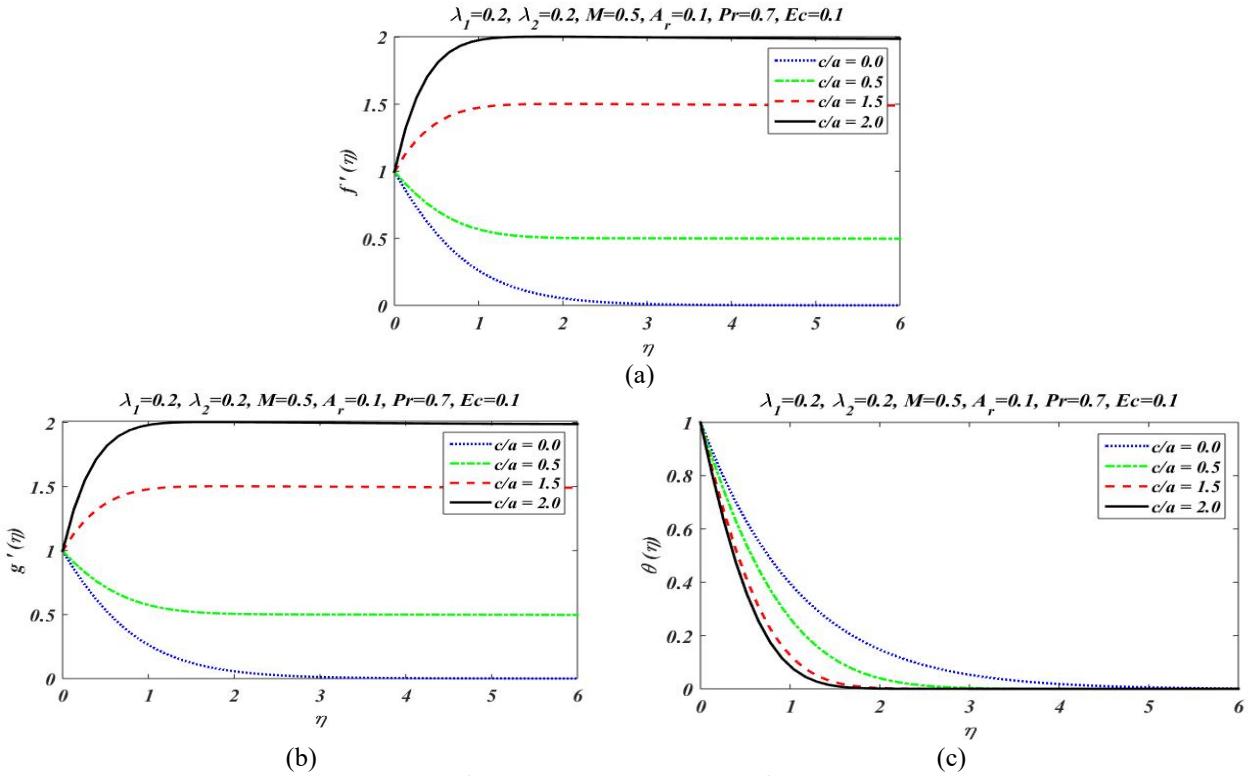

Fig. 4. Graphs of (a) Velocity profile $f^{'}(\eta)$ (b) Velocity profile $g^{'}(\eta)$ and (c) Temperature distribution $\theta(\eta)$ verses η for different values of c/a

In Figure 5(a)-(b) when $c/a = 0.2$ explained the result of Hartmann number M on velocity field $f'(\eta)$ & $g'(\eta)$. It is observed that the thickness of the momentum boundary layer is minimized as the value of M is enhanced. This is because of magnetic field proffers a force which is known as the Lorentz force. As Lorentz force is a resistive force which produces a resistance in fluid motion. In Figure 5 (c), present the performance of the temperature profile affects by the different value of M when other parameters Prandt $Pr = 0.7$, Eckert number $Ec = 0.1$ Archimedesnumber$Ar = 0.1, a/c = 0.2, \lambda_1 = 0.2, \lambda_2 = 0.2$ are being kept fixed. It is ceased that Thermal boundary layer thickness becomes thicker with the enhancement of M.

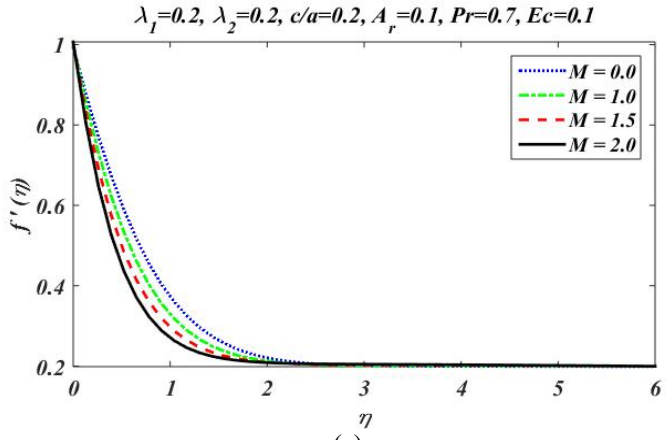

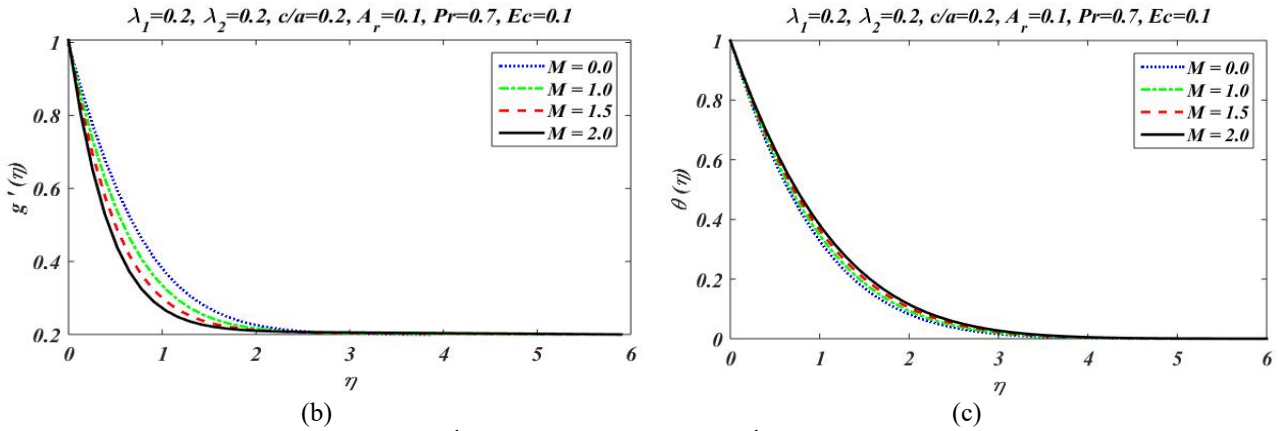

(b) (c)

Fig. 5. Graphs of (a) Velocity profile $f^{'}(\eta)$ (b) Velocity profile $g^{'}(\eta)$ and (c) Temperature distribution $\theta(\eta)$ verses η for different values of M

Figure 6(a)-(c) are represented to see the influence of Archimedes number $A_r$on velocity profile $f'(\eta)$ with respect to η. It shows that the temperature profile of Oldroyd-B fluid inclines by taking different values of Archimedes number $= 0.0 - 0.9$. It is observed that velocity $f'(\eta)$ goes down with an increment in the value of Archimedes number while $g^{'}(\eta)$ goes up as A_r is enhanced. The thermal boundary layer thickness achieved the maximum value at $A_r = 0.9$.

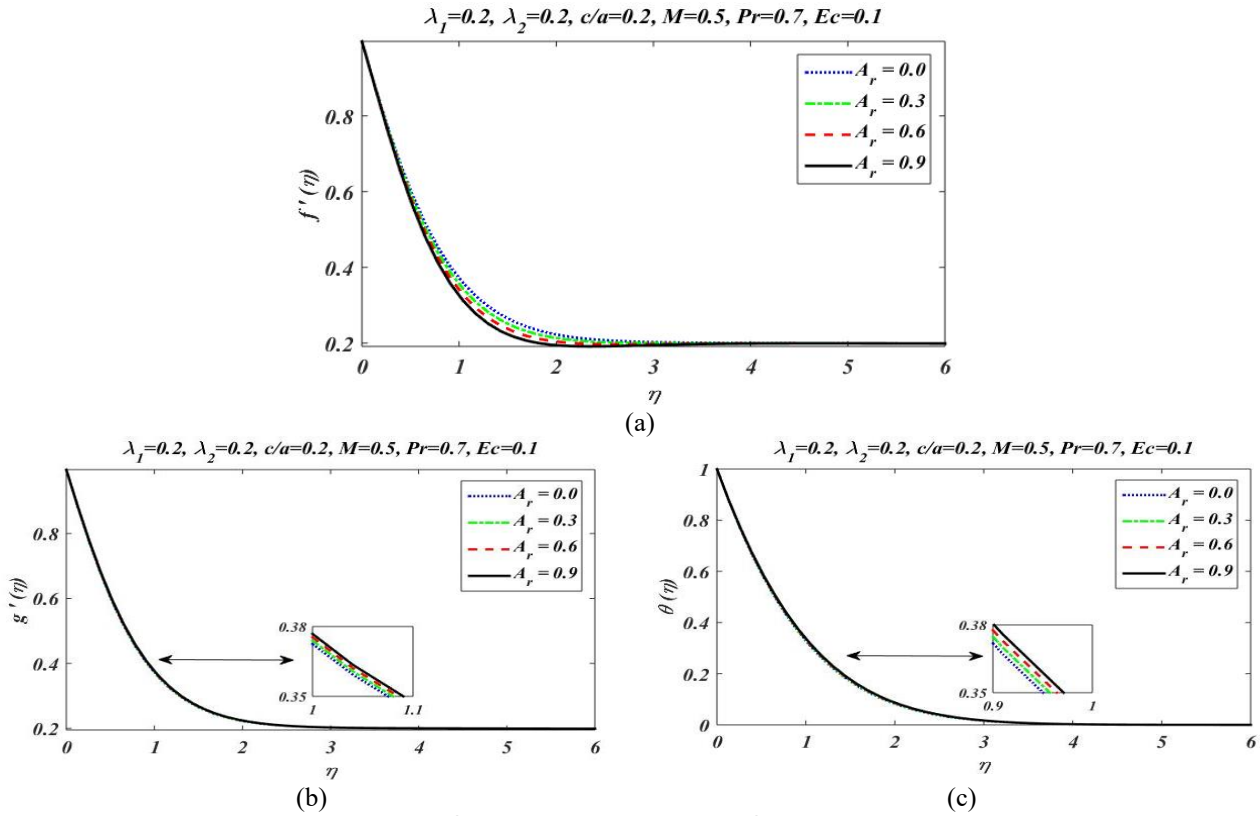

(a)

(b) (c)

Fig. 6. Graphs of (a) Velocity profile $f^{'}(\eta)$ (b) Velocity profile $g^{'}(\eta)$ and (c) Temperature distribution $\theta(\eta)$ verses η for different values of A_r

Figure 7 & Figure 8 illustrated the influences of dimensionless relaxation/retardation times (λ_1, λ_2) on the velocity components $f'(\eta)$ & $g'(\eta)$ for several values of c/a. In Figure 7(a)-(b) is quite clear that by increasing the value of relaxation time $\lambda_1$increases $f'(\eta)$& $g'(\eta)$ the when $c/a > 1$, then the behavior of velocity $f'(\eta)$ and $g'(\eta)$ and λ_1 is opposite i.e. velocity increases

when an increase in relaxation time λ_1. When λ_1 increases in both cases $c/a > 1$ & $c/a < 1$, the boundary layer thickness is increased. Moreover, Figure 8(a)-(b) shows that the retardation time λ_2 has an adverse effect on velocity $f'(\eta)$ & $g'(\eta)$ w.r.t relaxation time λ_1.

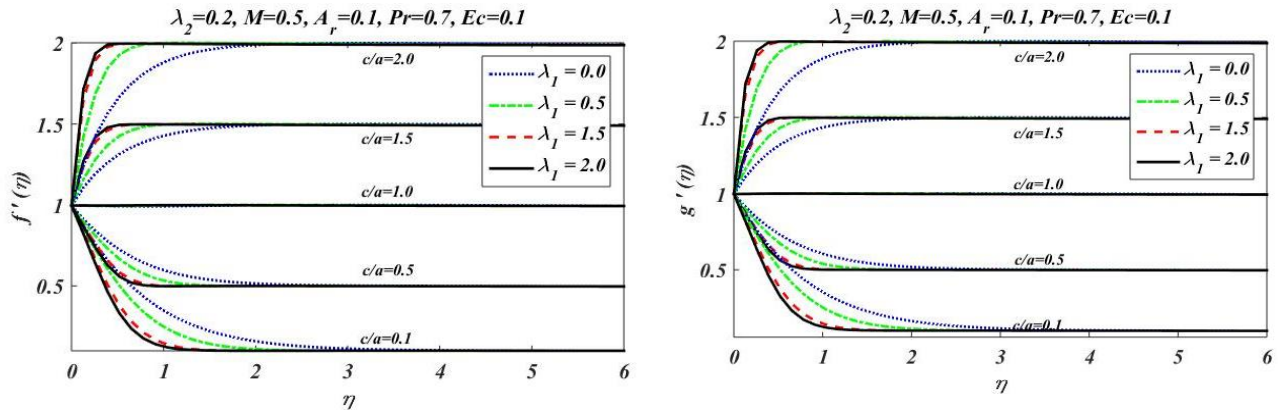

(a) (b)

Fig. 7. Influence of λ_1. on (a) Velocity profile $f'(\eta)$ (b) Velocity profile $g'(\eta)$ verses η for various values of $\frac{c}{a}$

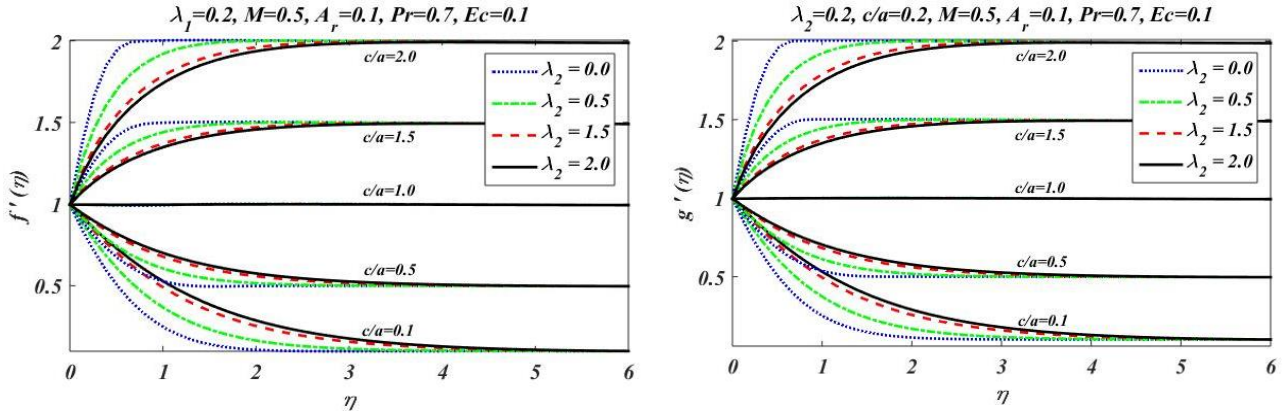

(a) (b)

Fig. 8. Influence of λ_2. on (a) Velocity profile $f'(\eta)$ (b) Velocity profile $g'(\eta)$ verses η for various values of $\frac{c}{a}$

Figure 9 illustrates the temperature distribution $\theta(\eta)$ in the presence of the Prandtl number. It confesses that the temperature of Oldroyd-B fluid stagnates by taking the different values of the Prandtl number between 0.7 and 7.0. It is concluded easily that both the thickness of the boundary layer and that of temperature are lessened because of increment in the respective value of Prandtl number. It is concluded that the maximum value of the temperature profile is attained at 0.7 when other parameters are constant. Prandtl number controls the momentum and thickness of the thermal boundary layer in the transfer of heat. When the Prandtl number is small, it shows that the thermal boundary layer thickness is large as compared velocity boundary layer thickness.

The physical behavior of temperature distribution θ(η) when several values of Eckert number Ec is considered keeping $Pr = 0.7,\ A_r = 0.1\,, c/a = 0.2, M = 0.2, \lambda_1 = 0.2, \lambda_2 = 0.2$ is shown in Figure 10. The analysis reveals an intriguing relationship between the temperature of Oldroyd-B fluid and the Eckert number (Ec). As the Eckert number increases, the temperature of the fluid also rises. This indicates that there is a direct proportionality between the energy dissipation at the surface (represented by the Eckert number) and the resultant increase in fluid temperature. Furthermore,

the graphical representation of the data demonstrates a specific trend: the thermal boundary layer thickness exhibits a minimum value when the Eckert number is at its lowest, which is 0.0. This observation suggests that when there is no energy dissipation at the surface ($Ec = 0.0$), the thermal boundary layer is at its thinnest. Conversely, as the Eckert number value increases, there is a noticeable enhancement in the thermal boundary layer thickness. This implies that greater energy dissipation at the surface leads to a thicker thermal boundary layer. The Eckert number, therefore, serves as a critical parameter influencing both temperature and thermal boundary layer characteristics in the context of Oldroyd-B fluid dynamics.

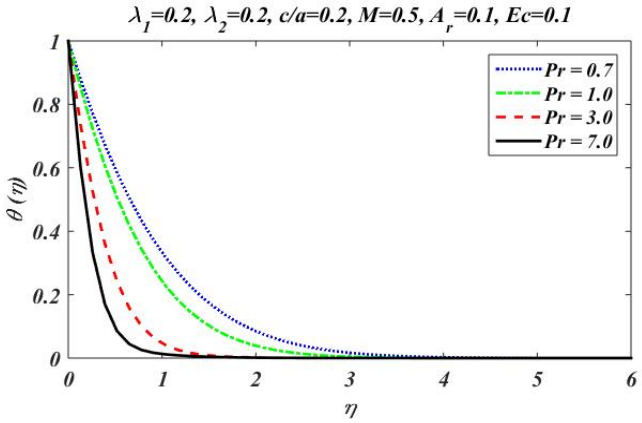

Fig. 9. Graphs of temperature distribution $\theta(\eta)$verses η for different values of Pr

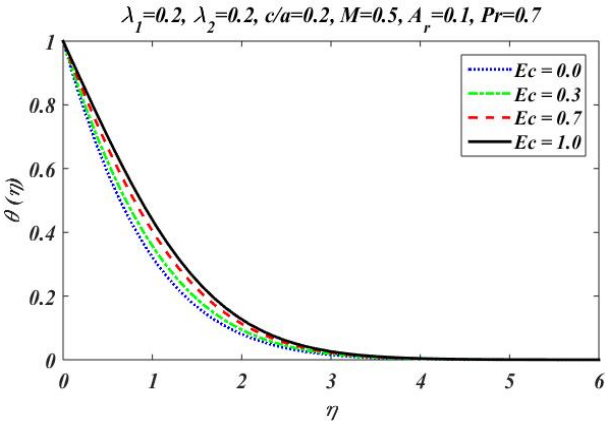

Fig. 10. Graphs of temperature distribution $\theta(\eta)$ verses η for different values of Ec

Table 1
Numerical values of $-\theta(0)$for different values of Pr, A_r and Ec

Pr	A_r	$Ec = 0.1$	$Ec = 0.5$	$Ec = 1.0$
0.7	1.0	1.0275	0.9313	0.8098
1.5		1.5395	1.3647	1.1428
3.0		2.2015	1.9116	1.5413
5.0		2.8435	2.4319	1.9036
7.0		3.3525	2.8392	2.1780
10.0		3.9774	3.3344	2.5025
100.0		10.566	8.4053	5.5371
0.5	0.0	0.8753	0.8100	0.7285
	0.2	0.8717	0.8049	0.7213
	0.5	0.8664	0.7973	0.7107
	1.0	0.8576	0.7846	0.6927
	2.0	0.8404	0.7592	0.6560
	3.0	0.8237	0.7336	0.6183
	5.0	0.7921	0.6820	0.5383

5. Conclusions

The study delves into the behaviour of fluid, specifically Oldroyd-B fluid, in a three-dimensional space, examining its interaction with a magnetic field and mixed convection during stagnation point flow. Initially, the fundamental governing equations are introduced to describe this complex fluid dynamics scenario. Subsequently, the focus shifts to analysing the transfer of heat and the flow characteristics over a stretching sheet oriented in the $xy-$direction at the stagnation point. To facilitate the analysis, a crucial step involves employing similarity transformations, which enable the conversion of the partial differential equations (PDEs) governing the fluid dynamics into ordinary

differential equations (ODEs). This transformation simplifies the mathematical treatment of the problem, making it more amenable to numerical methods. The numerical solution is obtained using the finite difference method, coupled with an iterative technique, which allows for the practical computation of the problem's intricate details. The results are then presented graphically, utilizing graphs to illustrate the influence of various dimensionless parameters on the system's behaviour. Several key findings emerge from this analysis:

i. It is observed that the thickness of the boundary layer increases with the retardation time.
ii. The momentum and thermal boundary layer thicknesses decrease as the stretching ratio increases.
iii. The magnetic field plays a crucial role in controlling the boundary layer thickness.
iv. Heat transfer is inversely related to the Eckert number; as the Eckert number increases, heat transfer is reduced.
v. An increase in the Prandtl number leads to a decrement in the temperature profile (η).

This comprehensive analysis of fluid dynamics, heat transfer, and magnetic field effects over a stretching sheet yields valuable insights into the behaviour of Oldroyd-B fluid. The findings have practical implications for various engineering and scientific applications where understanding boundary layer characteristics and heat transfer processes is crucial.

Acknowledgement
This research is not funded by any grant.

References

[1] Harris, John. "Rheology and non-Newtonian flow." (No Title) (1977).
[2] Khan, Sami Ullah, Nasir Ali, Muhammad Sajid, and Tasawar Hayat. "Heat transfer characteristics in oscillatory hydromagnetic channel flow of Maxwell fluid using Cattaneo–Christov model." *Proceedings of the National Academy of Sciences, India Section A: Physical Sciences* 89 (2019): 377-385. https://link.springer.com/article/10.1007/s40010-017-0470-6
[3] Nazeer, Mubbashar, Farooq Hussain, M. Ijaz Khan, Essam Roshdy El-Zahar, Yu-Ming Chu, and M. Y. Malik. "RETRACTED: Theoretical study of MHD electro-osmotically flow of third-grade fluid in micro channel." (2022): 126868. https://doi.org/10.1016/j.amc.2021.126868
[4] Zhao, Tie-Hong, M. Ijaz Khan, and Yu-Ming Chu. "Artificial neural networking (ANN) analysis for heat and entropy generation in flow of non-Newtonian fluid between two rotating disks." *Mathematical Methods in the Applied Sciences* 46, no. 3 (2023): 3012-3030. https://doi.org/10.1002/mma.7310
[5] Chu, Yu-Ming, B. M. Shankaralingappa, Bijjanal Jayanna Gireesha, Faris Alzahrani, M. Ijaz Khan, and Sami Ullah Khan. "RETRACTED: Combined impact of Cattaneo-Christov double diffusion and radiative heat flux on bio-convective flow of Maxwell liquid configured by a stretched nano-material surface." (2022): 126883. https://doi.org/10.1016/j.amc.2021.126883
[6] Khan, W. A., M. Irfan, and M. Khan. "An improved heat conduction and mass diffusion models for rotating flow of an Oldroyd-B fluid." *Results in physics* 7 (2017): 3583-3589. https://doi.org/10.1016/j.rinp.2017.08.068
[7] Zhang, Yan, Bo Yuan, Yu Bai, Yingjian Cao, and Yunpeng Shen. "Unsteady Cattaneo-Christov double diffusion of Oldroyd-B fluid thin film with relaxation-retardation viscous dissipation and relaxation chemical reaction." *Powder Technology* 338 (2018): 975-982. https://doi.org/10.1016/j.powtec.2018.07.049
[8] Khan, Sami Ullah, Sabir Ali Shehzad, and Sana Nasir. "Unsteady flow of chemically reactive Oldroyd-B fluid over oscillatory moving surface with thermo-diffusion and heat absorption/generation effects." *Journal of the Brazilian Society of Mechanical Sciences and Engineering* 41, no. 2 (2019): 72. https://link.springer.com/article/10.1007/s40430-019-1577-2
[9] Wang, Jing, M. Ijaz Khan, Waqar Azeem Khan, Syed Zaheer Abbas, and M. Imran Khan. "Transportation of heat generation/absorption and radiative heat flux in homogeneous–heterogeneous catalytic reactions of non-Newtonian fluid (Oldroyd-B model)." *Computer Methods and Programs in Biomedicine* 189 (2020): 105310. https://doi.org/10.1016/j.cmpb.2019.105310

[10] Hafeez, Abdul, Masood Khan, and Jawad Ahmed. "Flow of magnetized Oldroyd-B nanofluid over a rotating disk." *Applied Nanoscience* 10 (2020): 5135-5147. https://doi.org/10.1007/s13204-020-01401-2

[11] Khan, Sami Ullah, Sabir Ali Shehzad, and Sana Nasir. "Unsteady flow of chemically reactive Oldroyd-B fluid over oscillatory moving surface with thermo-diffusion and heat absorption/generation effects." *Journal of the Brazilian Society of Mechanical Sciences and Engineering* 41, no. 2 (2019): 72. https://doi.org/10.1007/s40430-019-1577-2

[12] Gudekote, Manjunatha, and Rajashekhar Choudhari. "Slip effects on peristaltic transport of Casson fluid in an inclined elastic tube with porous walls." *Journal of Advanced Research in Fluid Mechanics and Thermal Sciences* 43, no. 1 (2018): 67-80.

[13] Hamrelaine, Salim, Fateh Mebarek-Oudina, and Mohamed Rafik Sari. "Analysis of MHD Jeffery Hamel flow with suction/injection by homotopy analysis method." *Journal of Advanced Research in Fluid Mechanics and Thermal Sciences* 58, no. 2 (2019): 173-186.

[14] Soid, Siti Khuzaimah, Siti Nor Asiah Ab Talib, Nur Hazirah Adilla Norzawary, Siti Suzilliana Putri Mohamed Isa, and Muhammad Khairul Anuar Mohamed. "Stagnation Bioconvection Flow of Titanium and Aluminium Alloy Nanofluid Containing Gyrotactic Microorganisms over an Exponentially Vertical Sheet." *Journal of Advanced Research in Fluid Mechanics and Thermal Sciences* 107, no. 1 (2023): 202-218. https://doi.org/10.37934/arfmts.107.1.202218

[15] Bakar, Fairul Naim Abu, and Siti Khuzaimah Soid. "MHD stagnation-point flow and heat transfer over an exponentially stretching/shrinking vertical sheet in a micropolar fluid with a Buoyancy effect." *Journal of Advanced Research in Micro and Nano Engineering* 7, no. 1 (2022): 1-7. https://akademiabaru.com/submit/index.php/arnht/article/view/4502

[16] Shamshuddin, M. D., Kanayo Kenneth Asogwa, and M. Ferdows. "Thermo-solutal migrating heat producing and radiative Casson nanofluid flow via bidirectional stretching surface in the presence of bilateral reactions." *Numerical Heat Transfer, Part A: Applications* (2023): 1-20. https://doi.org/10.1080/10407782.2023.2191873

[17] Ahmed, AKM Muktadir, M. D. Shamshuddin, M. Ferdows, and Mohamed R. Eid. "Heat and mass transport through biaxial extending sheet with anisotropic slip and entropy/Bejan on the three-dimensional boundary layer hybrid nanofluid." *Proceedings of the Institution of Mechanical Engineers, Part E: Journal of Process Mechanical Engineering* (2022): 09544089221147394. https://doi.org/10.1177/09544089221147394

[18] Shamshuddin, M. D., S. O. Salawu, K. Ramesh, Vishwambhar S. Patil, and Pooja Humane. "Bioconvective treatment for the reactive Casson hybrid nanofluid flow past an exponentially stretching sheet with Ohmic heating and mixed convection." *Journal of Thermal Analysis and Calorimetry* 148, no. 21 (2023): 12083-12095. https://doi.org/10.1007/s10973-023-12465-x

[19] Salawu, S. O., E. I. Akinola, and M. D. Shamshuddin. "Entropy generation and current density of tangent hyperbolic Cu-C2H6O2 and ZrO2-Cu/C2H6O2 hybridized electromagnetic nanofluid: a thermal power application." *South African Journal of Chemical Engineering* 46 (2023): 1-11. https://doi.org/10.1016/j.sajce.2023.07.003

[20] Shamshuddin, M. D., F. Mabood, W. A. Khan, and Govind R. Rajput. "Exploration of thermal Péclet number, vortex viscosity, and Reynolds number on two-dimensional flow of micropolar fluid through a channel due to mixed convection." *Heat Transfer* 52, no. 1 (2023): 854-873. https://doi.org/10.1002/htj.22719

[21] Cao, Wenhao, Muhammad Madssar Kaleem, Muhammad Usman, Muhammad Imran Asjad, Musawa Yahya Almusawa, and Sayed M. Eldin. "A study of fractional Oldroyd-B fluid between two coaxial cylinders containing gold nanoparticles." *Case Studies in Thermal Engineering* 45 (2023): 102949. https://doi.org/10.1016/j.csite.2023.102949

[22] Asjad, Muhammad Imran, Rizwan Karim, Abid Hussanan, Azhar Iqbal, and Sayed M. Eldin. "Applications of fractional partial differential equations for MHD casson fluid flow with innovative ternary nanoparticles." *Processes* 11, no. 1 (2023): 218. https://doi.org/10.3390/pr11010218

[23] Yasir, Muhammad, Masood Khan, and Zaka Ullah Malik. "Analysis of thermophoretic particle deposition with Soret-Dufour in a flow of fluid exhibit relaxation/retardation times effect." *International Communications in Heat and Mass Transfer* 141 (2023): 106577. https://doi.org/10.1016/j.icheatmasstransfer.2022.106577

[24] Yasir, Muhammad, Masood Khan, Awais Ahmed, and Mahnoor Sarfraz. "Flow of Oldroyd-B nanofluid in non-inertial frame inspired by Cattaneo-Christov theory." *Waves in Random and Complex Media* (2023): 1-12. https://doi.org/10.1080/17455030.2023.2172626

[25] Kaleem, Muhammad Madssar, Muhammad Imran Asjad, Muhammad Usman, and Mustafa Inc. "Effects of natural convection flow of fractional Maxwell hybrid nanofluid by finite difference method." *Waves in Random and Complex Media* (2023): 1-16. https://doi.org/10.1080/17455030.2022.2164381

[26] Asjad, Muhammad Imran, Muhammad Usman, Taghreed A. Assiri, Arfan Ali, and ElSayed M. Tag-ElDin. "Numerical investigation of fractional Maxwell nano-fluids between two coaxial cylinders via the finite difference approach." *Frontiers in Materials* 9 (2023): 1050767. https://doi.org/10.3389/fmats.2022.1050767

[27] Ayub, Assad, Syed Zahir Hussain Shah, Muahmmad Imran Asjad, Musawa Yahya Almusawa, Sayed M. Eldin, and Magda Abd El-Rahman. "Biological interactions between micro swimmers and cross fluid with inclined MHD effects in a complex wavy canal." *Scientific Reports* 13, no. 1 (2023): 4712. https://doi.org/10.1038/s41598-023-31853-9

[28] Khan, Masood, Muhammad Yasir, Ali Saleh Alshomrani, Sivanandam Sivasankaran, Yaser Rajeh Aladwani, and Awais Ahmed. "Variable heat source in stagnation-point unsteady flow of magnetized Oldroyd-B fluid with cubic autocatalysis chemical reaction." *Ain Shams Engineering Journal* 13, no. 3 (2022): 101610. https://doi.org/10.1016/j.asej.2021.10.005

[29] Khan, Masood, Muhammad Yasir, Ali Saleh Alshomrani, Sivanandam Sivasankaran, Yaser Rajeh Aladwani, and Awais Ahmed. "Variable heat source in stagnation-point unsteady flow of magnetized Oldroyd-B fluid with cubic autocatalysis chemical reaction." *Ain Shams Engineering Journal* 13, no. 3 (2022): 101610. https://doi.org/10.1016/j.asej.2021.10.005

[30] Yasir, Muhammad, and Masood Khan. "Dynamics of heat transport in flow of non-linear Oldroyd-B fluid subject to non-Fourier's theory." *ZAMM-Journal of Applied Mathematics and Mechanics/Zeitschrift für Angewandte Mathematik und Mechanik* (2023): e202100393. https://doi.org/10.1002/zamm.202100393

[31] Yasir, Muhammad, and Masood Khan. "Dynamics of unsteady axisymmetric of Oldroyd-B material with homogeneous-heterogeneous reactions subject to Cattaneo-Christov heat transfer." *Alexandria Engineering Journal* 74 (2023): 665-674. https://doi.org/10.1016/j.aej.2023.05.065

[32] Sajid, M., Z. Abbas, T. Javed, and N. Ali. "Boundary layer flow of an Oldroyd-B fluid in the region of a stagnation point over a stretching sheet." *Canadian Journal of Physics* 88, no. 9 (2010): 635-640. https://doi.org/10.1139/P10-049

[33] Azeem Khan, Waqar, Masood Khan, and Rabia Malik. "Three-dimensional flow of an Oldroyd-B nanofluid towards stretching surface with heat generation/absorption." *PLoS One* 9, no. 8 (2014): e105107. https://doi.org/10.1371/journal.pone.0105107